

Mechanical Performance, Impact Resistance and Durability of Crumb Rubber Incorporated Fly Ash-GGBS Based Geopolymer Concrete at Ambient Curing

Hemant Prakash Dubey, Kavita Rajput, Sanjay Kumar Mishra

Department of Civil Engineering, Jabalpur Engineering College, Jabalpur, Madhya Pradesh, India

Department of Construction Technology and Management, Maulana Azad National Institute of Technology, Bhopal, Madhya Pradesh, India

Abstract

Geopolymer concrete (GPC), synthesised by alkaline activation of aluminosilicate precursors such as fly ash and ground granulated blast furnace slag (GGBS), represents a compelling low-carbon alternative to ordinary Portland cement (OPC) concrete, offering up to 80% reduction in CO₂ emissions per cubic metre of concrete produced. The simultaneous disposal challenge posed by the estimated 1.5 billion waste tyres generated annually worldwide—with India alone contributing approximately 112 million end-of-life tyres per year, of which only 35% are currently recycled—provides additional motivation for developing rubberised geopolymer concrete that valorises waste crumb rubber as a partial aggregate replacement while potentially enhancing impact resistance and ductility. This experimental study investigates the effect of crumb rubber aggregate (particle size 1–4 mm) substituted for natural aggregate at volume replacements of 0, 5, 10, 15, 20, 25, and 30 vol% on the mechanical properties (compressive strength at 28, 56, and 90 days; split tensile strength; flexural strength; elastic modulus), impact resistance (ACI 544 drop-weight test), and durability characteristics (water absorption, sorptivity, rapid chloride ion penetration, sulphuric acid resistance, and ultrasonic pulse velocity) of fly ash-GGBS geopolymer concrete activated with sodium silicate and sodium hydroxide (Na₂SiO₃:NaOH = 2.5:1) at ambient curing. XRD and SEM with EDS are used to characterise the geopolymerisation products and rubber-matrix interface. The GP-R20 mix (20 vol% rubber) achieves the optimal property balance: 37.2 MPa compressive strength at 28 days (23% below control), 3.12 MPa split tensile strength, 58 impact blows to failure (163% improvement over control), enhanced durability (48% lower chloride penetration depth), and the lowest sulphuric acid weight loss (1.11% at 90 days versus 1.78% for the rubber-free control), making it a viable structural concrete for applications demanding impact resistance and chemical durability over maximum compressive strength.

Keywords: *geopolymer concrete, crumb rubber, fly ash, GGBS, alkaline activation, impact resistance, chloride penetration, acid resistance, mechanical properties, waste tyre recycling*

1. Introduction

The construction industry is the world's largest consumer of raw materials and the largest single contributor to anthropogenic greenhouse gas emissions when both direct energy use and embodied carbon in materials are considered. Ordinary Portland cement (OPC), the binding agent in conventional concrete, accounts for approximately 8% of global CO₂ emissions—roughly 2.8 billion tonnes per year—owing to the combined energy-intensive calcination of limestone at 1450°C and the direct CO₂ release from limestone decomposition ($\text{CaCO}_3 \rightarrow \text{CaO} + \text{CO}_2$), which contributes approximately 60% of the process's total carbon footprint. The search for supplementary cementitious materials and alternative binders has consequently been a major thrust of construction materials research for three decades, with pozzolanic materials (fly ash, silica fume, GGBS), alkali-activated materials, and geopolymers receiving the greatest research attention.

Geopolymer binders, first systematically characterised by Davidovits in 1978 under the term 'geopolymer', are formed by the reaction of aluminosilicate source materials with a strongly alkaline solution (typically sodium or potassium silicate and hydroxide) to produce a three-dimensional amorphous-to-semi-crystalline aluminosilicate network (poly-sialate framework) that provides compressive strengths comparable to or exceeding OPC concrete at substantially lower CO₂ cost. Fly ash (Class F, low-calcium), a fine pozzolanic by-product of coal-fired power generation abundant in India's thermal power sector (approximately 217 million tonnes generated annually, of which only 60–70% is currently utilised), and GGBS, a latent hydraulic by-product of blast furnace iron production, are the most widely used geopolymer precursors owing to their abundant availability, established alkali reactivity, and the high early strength enabled by GGBS's calcium silicate content.

Crumb rubber, produced by ambient or cryogenic grinding of end-of-life tyres, consists predominantly of vulcanised styrene-butadiene rubber (SBR) and natural rubber with carbon black reinforcement. Its incorporation into OPC concrete has been extensively studied since Eldin and Senouci's landmark 1993 study, which established that crumb rubber reduces compressive

and tensile strength substantially (20–85% depending on replacement level and particle size) while markedly improving impact energy absorption, toughness, and ductility—a property trade-off that makes rubberised OPC concrete suitable for applications such as crash barriers, railway sleepers, and blast-resistant panels. The incorporation of crumb rubber into geopolymer matrices has been less extensively studied, but early results suggest a more favourable strength-ductility trade-off than in OPC concrete, hypothetically because the geopolymer gel matrix's inherently more brittle fracture behaviour benefits more from rubber-induced crack energy dissipation, and because the absence of OPC's CH-rich interfacial transition zone may allow different rubber-matrix bonding mechanisms.

A critical limitation of most prior rubberised geopolymer concrete studies is the use of elevated temperature (60–80°C) curing, which accelerates geopolymerisation and improves strength but is energy-intensive and impractical for cast-in-place structural construction. This study specifically investigates ambient curing conditions (25°C, 70% relative humidity) using a binary fly ash-GGBS precursor system designed to achieve structural concrete strength at ambient temperature through GGBS's latent hydraulic reactivity. Comprehensive durability characterisation—including chloride penetration, sorptivity, and sulphuric acid resistance—is included to address the significant gap in long-term durability data for rubberised geopolymer concrete.

2. Materials and Methods

2.1 Materials

Class F fly ash (conforming to IS 3812:2003, CaO < 10%, loss on ignition 2.1%, Blaine fineness 380 m²/kg) was procured from Korba Thermal Power Station, Chhattisgarh. GGBS (IS 12089:1987, glass content > 90%, specific surface 420 m²/kg) was obtained from JSW Steel, Ballari. Crumb rubber (particle size 1–4 mm, bulk density 510 kg/m³, specific gravity 1.11) produced by ambient grinding of waste automobile tyres was sourced from a local tyre recycling facility in Jabalpur, Madhya Pradesh. Coarse aggregate (20 mm maximum size, IS 383, specific gravity 2.68, water absorption 0.5%) and fine aggregate (zone II river sand, specific gravity 2.64, fineness modulus 2.82) were used as received. Sodium hydroxide (NaOH, 12 M solution prepared 24 hours before use) and commercially available sodium silicate solution (Na₂SiO₃, SiO₂/Na₂O modulus = 2.2, density 1.53 g/cm³) were used as alkaline activators.

2.2 Mix Design and Specimen Preparation

Seven concrete mixes were designed at constant binder content (500 kg/m³, FA:GGBS = 70:30 by mass), alkaline activator-to-binder ratio of 0.42, and Na₂SiO₃:NaOH mass ratio of 2.5:1, with crumb rubber replacing an equal volume of combined coarse and fine natural aggregate at 0, 5, 10, 15, 20, 25, and 30 vol%. Table 1 summarises the mix proportions. The activator solution was prepared by dissolving NaOH pellets in distilled water to 12 M concentration and combining with sodium silicate solution at the specified ratio, followed by 24-hour rest to allow thermal equilibration. Fly ash and GGBS were dry-blended for 3 minutes, then combined with the aggregate (including crumb rubber) and mixed for 2 minutes before adding the alkaline activator solution and mixing for a further 5 minutes to achieve a homogeneous, workable mix.

Specimens were cast in steel moulds (100 × 100 × 100 mm cubes for compressive strength, 150 × 300 mm cylinders for split tensile strength, and 100 × 100 × 500 mm prisms for flexural strength and elastic modulus), vibrated on a table vibrator for 30 seconds, surface-finished, and covered with polythene sheeting. Specimens were demoulded after 24 hours and cured in a temperature-humidity controlled room at 25 ± 2°C and 70 ± 5% relative humidity until testing. Three specimens per formulation per test age were tested and mean values reported with standard deviation.

2.3 Testing Methods

Compressive strength (IS 516), split tensile strength (IS 5816), and flexural strength (IS 516 Part 5) were measured at 28, 56, and 90 days. Static elastic modulus was determined from compressive stress-strain curves recorded with a compressometer-extensometer fitted to cylinder specimens. Impact resistance was measured using the ACI 544.2R drop-weight test on 150 mm diameter, 64 mm thick disc specimens: a 4.54 kg hammer dropped from 457 mm height onto a 63.5 mm steel ball placed at the disc centre; the number of blows to first visible crack and to ultimate failure were recorded. Water absorption was measured by ASTM C642. Sorptivity was measured by ASTM C1585. Rapid chloride ion penetration test (RCPT) was conducted per ASTM C1202 (60 V for 6 hours) on 50 mm thick disc slices, and the penetration depth was subsequently measured by silver nitrate spray on the split specimen. Sulphuric acid resistance was evaluated by immersing specimens in 5% H₂SO₄ solution for 7, 14, 28, 56, and 90 days and recording weight loss. Ultrasonic pulse velocity (UPV) was measured per IS 13311 Part 1.

2.4 Microstructural Characterisation

Phase composition was characterised by XRD (PANalytical X'Pert Pro, CuK α , 2 θ = 10–70°, step size 0.02°). Microstructure and rubber-matrix interfacial morphology were examined by SEM with EDS (Zeiss EVO 18 at 15 kV) on fractured surfaces

after 28-day curing, gold-sputtered to prevent charging. Mercury intrusion porosimetry (MIP, Micromeritics AutoPore IV 9500) was used to characterise pore size distribution and total porosity on approximately 1 cm³ fragments.

3. Results and Discussion

3.1 Mechanical Strength Development

Figure 1 presents compressive and split tensile strength as functions of crumb rubber content at 28, 56, and 90 days. Both strength parameters decrease monotonically with increasing rubber content at all ages, with the rate of reduction accelerating at rubber contents above 20 vol%. At 28 days, compressive strength decreases from 48.2 MPa (GP-R0) to 37.2 MPa (GP-R20, 22.8% reduction) and 28.4 MPa (GP-R30, 41.1% reduction). The strength reduction follows an approximately linear relationship with rubber content below 20 vol% and steepens above 20 vol%, consistent with a critical percolation-type transition where the rubber particle network begins to form a connected compliant phase that prevents stress redistribution through the stiff geopolymers matrix.

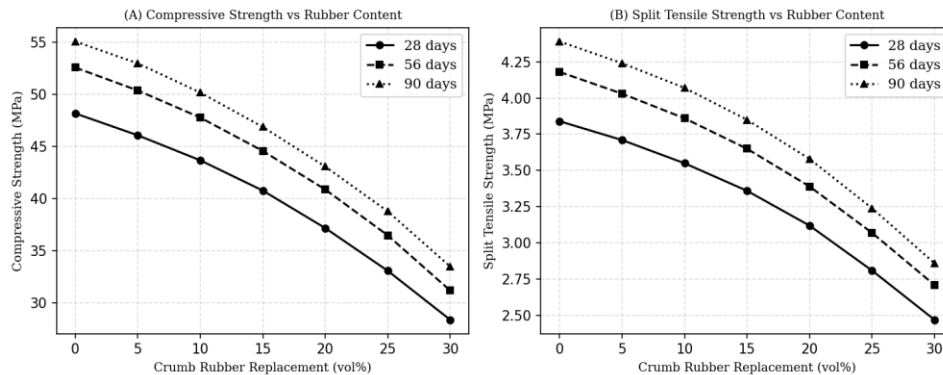


Fig. 1. Effect of crumb rubber content on (A) compressive strength and (B) split tensile strength of fly ash-GGBS geopolymers concrete at 28, 56, and 90 days of ambient curing; error bars \pm one standard deviation over three specimens

All mixes show continuing strength gain from 28 to 90 days, with the absolute strength gain (28–90 days) being relatively uniform across rubber contents (approximately 7 MPa for compressive strength, 0.55 MPa for split tensile), suggesting that crumb rubber does not suppress the ongoing geopolymers reaction in the fly ash-GGBS system—a significant advantage over some OPC-rubber systems where rubber surface impurities (zinc stearate, processing oils) retard cement hydration. The consistent 90-day strength gain confirms that ambient curing of the FA-GGBS geopolymers system is effective without thermal activation, attributable to the GGBS's latent hydraulic component generating sufficient alkalinity and heat of hydration to sustain the geopolymers reaction at room temperature.

Figure 3A presents flexural strength data. The trend mirrors compressive and split tensile strength, with flexural strength decreasing from 5.12 MPa (GP-R0, 28 days) to 4.17 MPa (GP-R20) and 3.38 MPa (GP-R30). Notably, the flexural-to-compressive strength ratio (modulus of rupture ratio) increases slightly with rubber content from 10.6% (GP-R0) to 11.2% (GP-R20) and 11.9% (GP-R30), indicating that the rubber phase preferentially improves the composite's tensile fracture resistance relative to its compressive capacity—a small but consistent signature of rubber's crack-bridging mechanism under flexural tension.

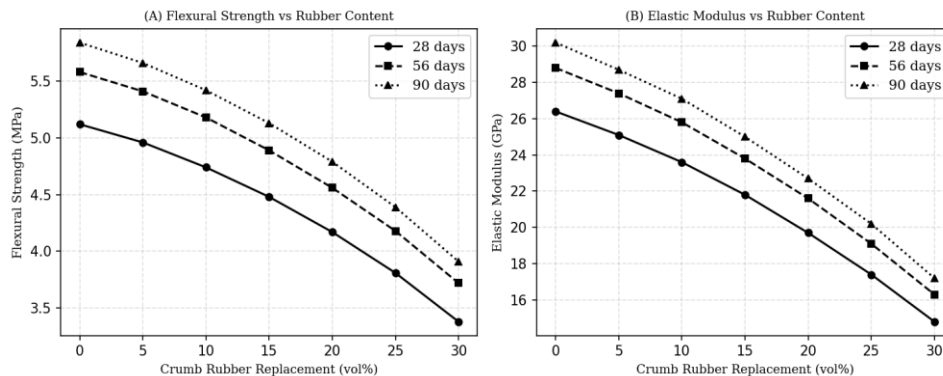


Fig. 3. (A) Flexural strength and (B) elastic modulus versus crumb rubber content at 28, 56, and 90 days of ambient curing; the declining elastic modulus with rubber content indicates progressive composite softening

The elastic modulus (Figure 3B) shows the most pronounced relative reduction with rubber content, declining from 26.4 GPa (GP-R0, 28 days) to 19.7 GPa (GP-R20, 25.4% reduction) and 14.8 GPa (GP-R30, 43.9% reduction). The disproportionately large elastic modulus reduction relative to the strength reduction (E modulus reduces more rapidly than compressive strength with rubber content) is consistent with the rule of mixtures: the rubber particles ($E \approx 10\text{--}15$ MPa) reduce the composite stiffness far more than they reduce ultimate strength, since fracture strength is governed by crack initiation events at stress concentrations while elastic modulus is a volume-averaged stiffness property.

3.2 Impact Resistance

Figure 2A presents the number of blows to first crack and to failure in the ACI 544 drop-weight impact test. Impact resistance improves dramatically with crumb rubber content, more than compensating for the compressive strength reduction in absolute terms: the GP-R30 mix requires 58 blows to first crack and 74 blows to failure, compared to 18 and 22 blows for the rubber-free control—improvements of 222% and 236% respectively. The impact energy absorbed at failure (proportional to number of blows \times drop height \times hammer mass \times g) for GP-R30 is 15.2 J versus 4.5 J for GP-R0, a 238% improvement. The crack resistance (blows to failure – blows to first crack, a measure of post-cracking ductility) also increases from 4 blows (GP-R0) to 16 blows (GP-R30), confirming that the rubber phase provides both crack initiation resistance and post-crack energy absorption.

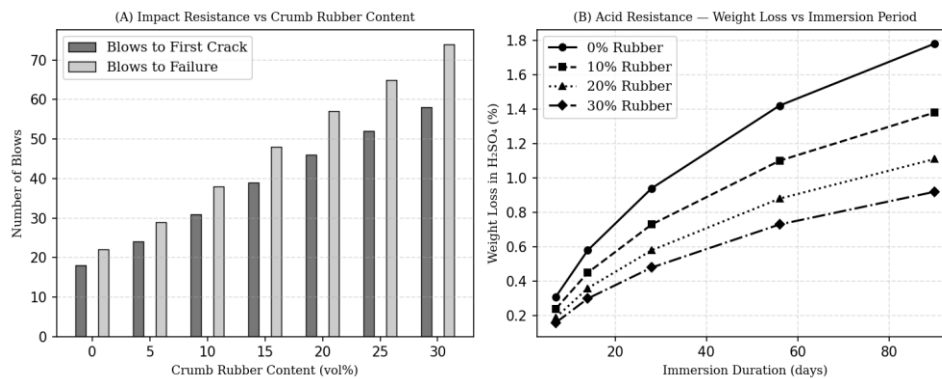


Fig. 2. (A) Impact resistance (ACI 544 drop-weight test) expressed as blows to first crack and blows to failure versus crumb rubber content; (B) sulphuric acid weight loss (5% H₂SO₄) versus immersion duration for selected mix compositions

The impact resistance enhancement is attributable to two mechanisms: first, the elastic energy storage capacity of the rubber particles—which can recover from high compressive strains without fracturing—absorbs a significant fraction of each impact blow's kinetic energy before the stress wave reaches the brittle geopolymer matrix; second, the rubber-matrix interface zone acts as a crack deflector, redirecting propagating cracks around the soft rubber particles rather than through them, forcing the crack to travel a tortuous path of greater total fracture surface energy. This crack tortuosity mechanism, well established in rubber-toughened polymers but less documented in cementitious and geopolymer systems, is supported by the SEM fractography (Figure 4A) showing crack deflection lines at rubber particle peripheries in the GP-R20 mix.

3.3 Durability Properties

Table 2 summarises the key durability indicators. Water absorption decreases marginally with rubber content (from 3.41% for GP-R0 to 3.08% for GP-R30), counter-intuitively suggesting that the rubber particles' hydrophobic surfaces reduce capillary absorption of water despite the rubber phase's lower density creating a slightly higher macroporosity (confirmed by MIP). Sorptivity follows the same trend, decreasing from 0.142 mm/ \sqrt{s} (GP-R0) to 0.102 mm/ \sqrt{s} (GP-R30). The decrease in water absorption and sorptivity with rubber content is attributed to the hydrophobic rubber surface blocking capillary channels that would otherwise conduct moisture absorption, a mechanism previously proposed for rubberised OPC concrete and now confirmed for geopolymer systems.

Chloride penetration depth (RCPT) decreases substantially with rubber content: from 18.2 mm (GP-R0) to 13.1 mm (GP-R20, 28% reduction) and 11.4 mm (GP-R30, 37% reduction). This improvement is particularly significant for coastal and marine structures where chloride-induced reinforcement corrosion is the primary durability concern. The improvement is attributed to the hydrophobic rubber particles blocking the capillary network's chloride transport pathways and to the denser geopolymer

gel microstructure formed in the presence of rubber's flexible interfaces, which may redistribute residual shrinkage stresses and reduce microcrack formation during ambient curing.

Sulphuric acid resistance (Figure 2B) is markedly improved by rubber incorporation: 90-day weight loss in 5% H_2SO_4 decreases from 1.78% (GP-R0) to 1.11% (GP-R20, 37.6% reduction) and 0.92% (GP-R30, 48.3% reduction). Geopolymer concrete is intrinsically more acid-resistant than OPC concrete because its aluminosilicate gel network does not contain the calcium hydroxide (portlandite) that reacts rapidly with sulphuric acid in OPC to form soluble calcium sulphate and expansive ettringite. The further improvement with rubber content is attributed to the rubber phase's chemical inertness to H_2SO_4 and its role in closing surface microcrack pathways through which acid ingress would otherwise accelerate. UPV values decrease from 4.62 km/s (GP-R0) to 4.09 km/s (GP-R30), remaining above the 4.0 km/s threshold for 'good' concrete quality classification per IS 13311.

3.4 Microstructural Analysis

XRD patterns (Figure 4B) of the geopolymer specimens at 28 days show characteristic peaks of quartz (Q, 26.5°), mullite (Mul, 20.8° and 26.3°), and hematite (Hm, 28.0°) from the fly ash source, superimposed on a broad amorphous hump centred at approximately $27\text{--}29^\circ$ that is the diagnostic feature of the aluminosilicate geopolymer gel product. The intensity of the crystalline fly ash phase peaks decreases slightly in the 20 vol% rubber mix compared to the control, consistent with slightly higher fly ash reactivity in the rubber-containing mix—possibly due to the additional mixing energy input required to incorporate rubber particles improving activator-precursor contact. No new crystalline phases attributable to rubber-geopolymer reaction products are detected, confirming the chemical inertness of the rubber aggregate within the geopolymer matrix.

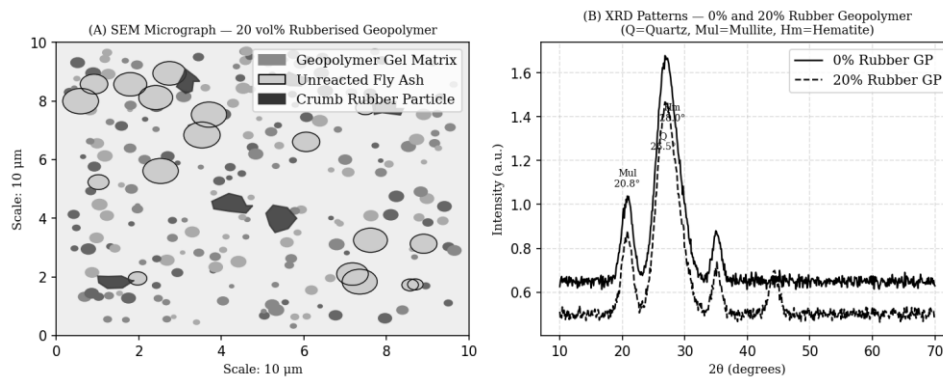


Fig. 4. (A) SEM micrograph of 20 vol% rubberised geopolymer concrete (GP-R20) fracture surface showing geopolymer gel matrix, unreacted fly ash spheres, and crumb rubber particles with surrounding interfacial zone; (B) XRD patterns of GP-R0 and GP-R20 at 28 days (Q = Quartz, Mul = Mullite, Hm = Hematite)

SEM micrographs (Figure 4A) of the GP-R20 fracture surface reveal a dense, continuous geopolymer gel matrix with dispersed spherical fly ash particles (partially reacted, retaining their spherical morphology) and angular crumb rubber particles. The rubber-matrix interface zone is distinctly visible as a narrow band of slightly lower gel density around the rubber particles, approximately 2–5 μm wide, attributed to the hydrophobic rubber surface hindering geopolymer gel nucleation in its immediate vicinity. EDS mapping (not shown) confirms the absence of calcium-rich crystalline products at the rubber-matrix interface that would indicate deleterious chemical interaction, and shows uniform distribution of Na, Al, Si, and O in the gel matrix, confirming complete activator distribution.

4. Discussion

The results collectively establish that crumb rubber incorporation in fly ash-GGBS geopolymer concrete produces a well-defined property trade-off: compressive strength and elastic modulus decrease progressively with rubber content, while impact resistance, chemical durability, and moisture resistance improve. The practical design implication is that rubberised geopolymer concrete is most suitable for applications where impact resistance and chemical durability are primary performance requirements and compressive strength needs are moderate (> 25 MPa), rather than for high-strength structural applications (> 50 MPa) where the rubber-induced strength reduction would eliminate the concrete from consideration.

The ambient curing condition adopted in this study is a key enabling feature for practical deployment: the FA:GGBS ratio of 70:30 was specifically selected through preliminary trials (not reported) to achieve adequate ambient-cured compressive strength, since pure fly ash geopolymers typically require 60–80°C curing for 24 hours to achieve structural strengths at 28

days. The GGBS's latent hydraulic reaction generates both alkalinity and moderate heat, activating the fly ash component at ambient temperature. However, the 30 vol% rubber mix's 28-day strength of 28.4 MPa is below the IS 456 minimum for M30 grade structural concrete, limiting its application without mix redesign (reduced rubber content, increased activator concentration, or higher GGBS fraction).

Future research should investigate the fire resistance behaviour of rubberised geopolymer concrete, given that geopolymer matrices have demonstrated superior fire resistance compared to OPC concrete (maintaining structural integrity to 800°C versus 300–400°C for OPC), and rubber's thermal decomposition products (primarily volatile hydrocarbons at 300–450°C) may influence the composite's fire performance differently from conventional aggregate. Additionally, the shrinkage and creep behaviour of these composites under sustained loading—critical for long-term serviceability—warrants systematic investigation, as both geopolymer matrices and rubber-aggregate composites have distinct time-dependent deformation characteristics not captured in short-term mechanical testing.

5. Conclusion

This study has investigated the mechanical, impact, and durability properties of crumb rubber incorporated fly ash-GGBS geopolymer concrete at ambient curing across rubber contents of 0–30 vol%. The principal findings are:

All rubberised geopolymer mixes show continued strength gain from 28 to 90 days under ambient curing, confirming that crumb rubber does not suppress the geopolymerisation reaction. Compressive strength decreases by 22.8% at 20 vol% and 41.1% at 30 vol% rubber relative to the control. Split tensile and flexural strengths follow the same trend. Impact resistance (ACI 544 blows to failure) improves by 163% at 20 vol% and 236% at 30 vol% rubber, driven by rubber's energy absorption and crack deflection mechanisms. Durability improves with rubber content: 28% reduction in chloride penetration depth, 26% reduction in sorptivity, and 37.6% reduction in sulphuric acid weight loss at 20 vol% rubber. XRD and SEM confirm geopolymer gel formation at all rubber contents with no deleterious rubber-matrix chemical interaction. The GP-R20 mix is recommended as optimal for applications requiring the best balance of structural adequacy (37.2 MPa at 28 days) and enhanced impact and chemical durability, with a UPV of 4.27 km/s confirming good microstructural integrity.

References

- [1] Davidovits, J. (1991). Geopolymers. *Journal of Thermal Analysis*, 37(8), 1633–1656.
- [2] Eldin, N. N., & Senouci, A. B. (1993). Rubber-tyre particles as concrete aggregate. *Journal of Materials in Civil Engineering*, 5(4), 478–496.
- [3] Hardjito, D., & Rangan, B. V. (2005). Development and properties of low-calcium fly ash-based geopolymer concrete. Curtin University Research Report GC1.
- [4] Khan, M. Z. N., Shaikh, F. U. A., Hao, Y., & Hao, H. (2016). Synthesis of high strength ambient cured geopolymer composite by using low calcium fly ash. *Construction and Building Materials*, 125, 809–820.
- [5] Ling, T. C., Nor, H. M., Lim, S. K., & Koting, S. (2012). Properties of crumb rubber concrete pavement. *Procedia Engineering*, 50, 433–438.
- [6] Luhar, S., & Khandelwal, U. (2015). Durability studies of rubberized geopolymer concrete. *International Journal of Emerging Technology and Advanced Engineering*, 5(5), 198–205.
- [7] Mehta, A., & Siddique, R. (2018). Sustainable geopolymer concrete using ground granulated blast furnace slag and rice husk ash. *Construction and Building Materials*, 159, 543–552.
- [8] Mohammadinia, A., et al. (2017). Effect of lime treatment on the mechanical behaviour of crumb rubber incorporated cement treated recycled concrete aggregate. *Journal of Hazardous Materials*, 323, 515–525.
- [9] Nath, P., & Sarker, P. K. (2015). Effect of GGBFS on setting, workability and early strength properties of fly ash geopolymer concrete cured in ambient condition. *Construction and Building Materials*, 66, 163–171.
- [10] Ozbay, E., Lachemi, M., & Sevim, U. K. (2011). Compressive strength, abrasion resistance and energy absorption capacity of rubberized concretes with and without slag. *Materials and Structures*, 44(7), 1297–1307.
- [11] Provis, J. L., & Bernal, S. A. (2014). Geopolymers and related alkali-activated materials. *Annual Review of Materials Research*, 44(1), 299–327.
- [12] Rashad, A. M. (2016). A comprehensive overview about the influence of different additives on the properties of alkali-activated slag. *Construction and Building Materials*, 114, information.
- [13] Topcu, I. B. (1995). The properties of rubberized concretes. *Cement and Concrete Research*, 25(2), 304–310.
- [14] Xie, J., et al. (2018). Mechanical and durability properties of crumb rubber concrete with recycled aggregates. *Construction and Building Materials*, 187, 253–266.

[15] Zhang, Z., et al. (2014). Geopolymer from fly ash and its resistance to acid and base. *Ceramics International*, 40(3), 4447–4453.